Nick Hatz*, Anton Averin and Julien Lecompagnon

Automated non-destructive internal corrosion detection on radioactive drums (ZIKA)

https://doi.org/10.1515/kern-2025-0101
Received December 1, 2025; accepted March 4, 2026;
published online May 6, 2026

Abstract: Against the backdrop of extended storage times in German interim storage facilities and the increase in low- and medium-level radioactive waste, monitoring container integrity is of critical importance. The ZIKA (Automated non-destructive internal corrosion detection on radioactive drums/15S9446A) research project, carried out as part of the FORKA funding initiative, presents an automated system for non-destructive testing (NDT) of radioactive waste drums. The primary goal is the reliable early detection of internal corrosion in order to identify safety risks before the integrity of the containers is compromised by externally visible degradation. As a further development of the predecessor project EMOS, the system architecture has been optimized for mobile use in a compact 10-foot container. The novel design integrates complex lifting mechanisms and robotics to ensure complete inspection of the entire drum surface, including the bottom. The multi-sensory approach combines laser scanners for topographic mapping, smart cameras for detecting external defects, and active thermography for identifying internal corrosion. Experimental validations by the Federal Institute for Materials Research and Testing (BAM) showed that laser thermography is more robust and reliable in defect detection than flash thermography. Machine learning algorithms were implemented for data analysis, with random forest models achieving the highest accuracy in defect classification and artifact suppression. The ZIKA system thus represents a significant contribution to increasing long-term safety standards in nuclear interim storage facilities.

Keywords: radioactive waste management; non-destructive testing (NDT); automated inspection systems; active thermography; corrosion detection; machine learning

***Corresponding author: Nick Hatz**, Karlsruher Institut für Technologie (KIT), Gotthard-Franz-Straße 3, 76131 Karlsruhe, Germany, E-mail: nick.hatz@kit.edu. https://orcid.org/0009-0001-3671-5468
Anton Averin and Julien Lecompagnon, Bundesanstalt für Materialforschung und -prüfung (BAM), Unter den Eichen 87, 12205 Berlin, Germany. https://orcid.org/0009-0000-3088-1919 (A. Averin). https://orcid.org/0000-0001-8614-3296 (J. Lecompagnon)

1 Introduction

Germany currently has more than 120,000 cubic meters of low- and medium-level radioactive waste with negligible heat generation, and this volume is set to increase further in the coming years (Bundesgesellschaft für Endlagerung 2023). This waste accounts for 90 % of all radioactive waste and is mainly stored in 200-L drums. The designated storage facilities consist of interim storage sites, which make up the majority, and state collection points, where small-scale producers from industry, research, and medicine are required by German law to deliver their waste. The low- and medium-level radioactive waste comes mainly from the dismantling and operation of nuclear power plants. (BASE 2024; Bundesgesellschaft für Endlagerung 2019).

The Konrad final repository, scheduled for completion in 2030, is intended for the final storage of this waste. However, it should be noted that, on the one hand, storage is a time-consuming process that will take several years and, on the other hand, a certain amount of radioactive waste will not yet have been removed from the structures to be dismantled by that date. As a result of these factors, there is an unplanned amount of low- and medium-level radioactive waste in interim storage sites throughout Germany. Statistical analyses show that just under 40 % of the waste in interim storage was stored before the turn of the millennium. In terms of integrity, special focus must be placed on waste that was already in interim storage before 1990. This waste accounts for a significant 13 % of all waste in interim storage and has already been stored for over 30 years. The early years of interim storage were a particularly critical factor, as some of the drums were stored in non-air-conditioned halls and the conditioning of the waste was not state-of-the-art. Humidity, temperature fluctuations, and other weather conditions could have significantly compromised the integrity of the low- and medium-level radioactive waste drums. In terms of internal corrosion, factors such as residual moisture in the drums and air pockets were a critical breeding ground for damage.

As part of the funding initiative „FORKA – Forschung für den Rückbau kerntechnischer Anlagen“ the Karlsruhe Institute of Technology (KIT) is working with project partners from the Bundesanstalt für Materialforschung und -prüfung (BAM), Kraftanlagen Heidelberg GmbH (KAH), and

the Landessammelstelle Berlin (ZRA) to develop an automated drum inspection system based on non-destructive testing methods as part of the ZIKA project. The overall goal of the ZIKA research proposal is to automatically detect internal corrosion in radioactive drums using non-destructive testing (NDT). These new findings will be combined with the previous research results of the predecessor project EMOS (Development of a Mobile and Automated Optical System for the Inspection of Radioactive Waste Drums/15S9420), which dealt with external damage to drums. This will enable the detection of internal corrosion and possible internal sources of damage before they become a safety issue. Until now, internal corrosion could only be detected when, for example, blisters formed on the paintwork of the drum container or external changes to the surface became apparent. However, once internal damage is visible externally, the integrity of the damaged drum container is no longer guaranteed, which has significant consequences. Early detection before integrity is compromised is therefore particularly important for the safe storage of radioactive waste.

In contrast to damage to containers for low- and medium-level radioactive waste caused by external corrosion, damage caused by internal corrosion is generally not easy to detect. Information on the current condition of the container interior, in particular on the condition of the corrosion protection layer, is not always available. Statements about the composition or condition of the waste in individual containers can only be made if sufficient documentation (i.e., information about the container and the corrosion protection used, the origin and type of waste, the conditioning process, and the duration and conditions of storage) is available for the container in question. This documentation, especially for old containers, often shows considerable deficiencies or is not available at all. Containers for which a potential hazard due to internal corrosion cannot be ruled out with certainty by visual inspection must be subjected to further examination. In order to ensure the greatest possible safety for the environment and, in particular, for personnel, non-destructive determination of the container condition is desirable.

However, the detection of corrosion under coating still poses a challenge for non-destructive testing (NDT) techniques. As part of the project, several NDT methods such as thermography, ultrasound, laser vibrometry, magnetic flux leakage measurement, and eddy current were compared on suitable test specimens to determine their suitability for detecting corrosion on the reverse side. Thermography achieved the best results.

For thermographic examinations, the test object is heated or warmed up. Heating can be either impulsive or periodic, or the object's own heat can be used if a container is already warm when it comes out of storage. In the subsequent cooling phase, an infrared camera is used to observe the temperature distribution on the surface of the component. If there are defects in the material (blisters, cavities, cracks, delaminations, etc.), the heat flow is disrupted, which becomes visible on the surface as temperature differences. The temperature differences can be detected and evaluated using the thermography camera. The advantages of thermography are that it is performed in real time and without contact, and that a large area can be inspected in a short time. Experience with the thermographic inspection of multilayer systems is available from previous BAM project activities. On the one hand, polymer layers on concrete (OSS) were examined with the aim of determining the layer thickness without contact. This joint project resulted in both a fully functional demonstrator and powerful software for analyzing the temperature profile of multilayer systems during pulsed heating (Altenburg et al. 2018; Antons 2019; Bernegger et al. 2020; Schlichting et al. 2012). This software allows the determination of layer thicknesses as well as thermal transition resistances for at least theoretically arbitrary material combinations. On the other hand, there were several projects on the thermographic quantification of spot welded joints after pulsed heating (Jonietz et al. 2015; Matthies 1998). These involve a two- or three-layer system of steel-welded lens-steel.

The ZIKA research project can be divided into three main areas: non-destructive testing methods, construction of the demonstrator, and proving practical feasibility.

The aim of KIT-TMB is the overall design and construction of the inspection unit, the technical implementation of the tests, and the assembly of the components. The inspection unit is designed so that it can be transportable and removed after use in a controlled area.

The ZIKA research and development project is funded by the German Federal Ministry of Research, Technology, and Space.

2 Concept

The following chapters describe the concepts, fundamentals, and components of the ZIKA research and development project.

2.1 Predecssor project EMOS

The planning is based on the results of the EMOS research and development project. The aim was to develop an automated drum inspection system that enables the current

condition of individual drums to be determined, documented, and reproduced in exactly the same way. EMOS is a mobile inspection unit that remotely and automatically captures images of the entire surface of a drum, including its lid and base, analyzes them, stores them electronically, and outputs the results in the form of an inspection report. This allows recurring inspections of the drum inventory in a temporary storage facility to be carried out under consistently identical test conditions. A key advantage is the possibility of performing the inspection remotely in order to reduce the radiation dose to employees on site.

The optical evaluation and presentation of the results by specially developed software ensures a more accurate inspection and analysis of the drum surfaces than is possible with manual and visual inspections, as are currently performed in interim storage facilities. Continuous monitoring of stored drums is made easier, and the tracing of possible damage development by comparing archived measurement results is a novel and powerful tool that helps to increase and ensure the safety aspects of interim storage in the long term. External corrosion damage can thus be detected at a very early stage and the loss of integrity of the storage containers can be counteracted by taking appropriate measures. The research and development work within the EMOS project has thus contribute to increasing the safety of extended interim storage.

The system is based on a 20-foot high-cube container (shown in Figure 1 (A)), which houses all the technology. After the barrel to be tested is placed on the external roller conveyor belt, the roller door opens and moves onto the turntable (shown in Figure 1 (B)).

There, the barrel is first centered and then the lid and jacket are detected by light section sensors and cameras. The turntable rotates so that the entire circumference can be detected (Figure 2 (A)). After the jacket and lid have been scanned, the barrel moves on to the barrel tilting system. There, it is tilted by 90°, so that the bottom faces the sensors that previously scanned the jacket. To maintain the same distance as before, the measuring technology is suspended from a linear unit that moves up to 900 mm (Figure 2 (B)).

Once the barrel has been scanned, it is returned to the loading point and the software evaluates the collected data. First, a height map is generated, showing where there are bumps or dents on the barrel (Figure 3 (A)). Based on the geometry it can be determined whether existing deformations are critical or not. The second component of the data evaluation is an evaluation of the images. This involves classifying the percentage of undamaged areas, reflections, primer, paint spots, light dirt, dark dirt, and corrosion (Figure 3 (B)).

This software also forms the basis for the evaluation process in ZIKA but is adapted and expanded for this purpose.

2.2 ZIKA prototype

One of the fundamental goals of ZIKA is to house the system in a smaller container than EMOS. This makes the system more mobile and allows it to be used in more temporary storage facilities, as a 20-foot container does not fit everywhere. The aim was therefore to use a 10-foot high-cube container as the basis for planning. The component in EMOS that requires the most space is the drum tilting system. For this reason, the focus was on selecting a more space-saving method in the new container to make the bottom visible. Initially, there were two concepts to choose from: 1. The drum is moved into a drum gripper and then lifted with a lift so that the bottom is exposed (Figure 4 (A)); 2. The drum is moved into a drum gripper using lifting columns so that the

Figure 1: EMOS inspection unit. (A) EMOS container, (B) Turntable with barrel centering device.

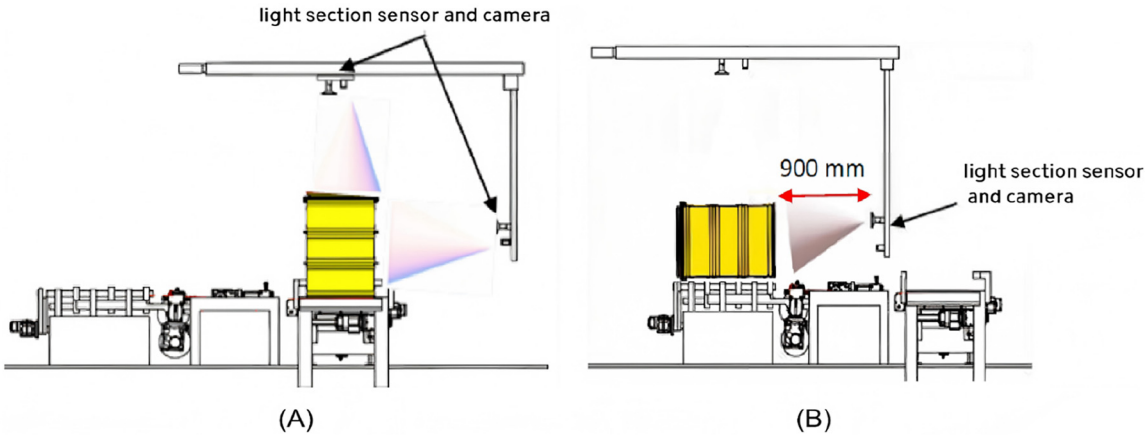

Figure 2: Schematic of the inner workings of EMOS. (A) Barrel wall & lid detection, (B) Bottom detection.

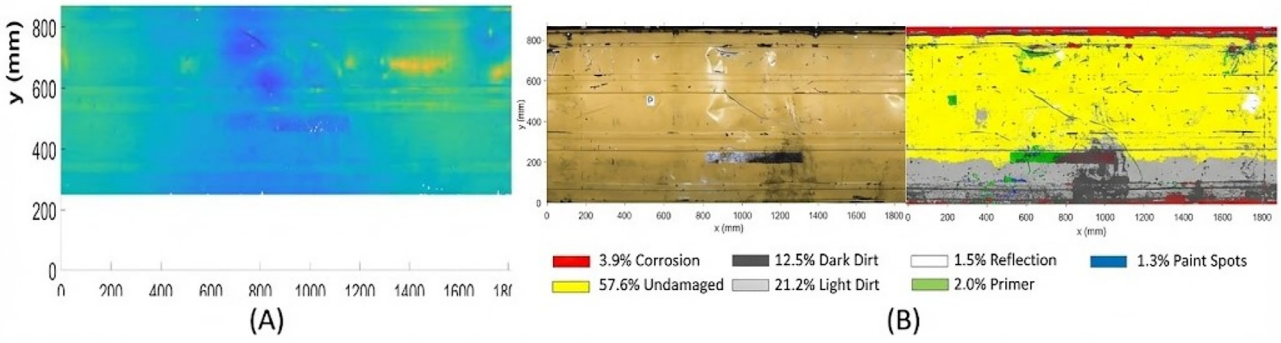

Figure 3: Optical inspection result. (A) Elevation map, (B) Image analysis.

bottom is exposed (Figure 4 (B)). The project team opted for the second variant which became increasingly detailed in the course of the project, up to the current status shown in Figure 4 (C).

3 Measuring system

For ZIKA three different measurements elements are in use:
- Laser to create evaluation map
- Smart camera for damage detection
- Thermography for inner corrosion detection

3.1 Laser and smart camera

As stated before, a laser (the same as in EMOS) is in use to create the evaluation map like in Figure 3 (A). Deviations from the original shape may indicate dents and bumps that can lead to critical damage over time.

To identify damages on the outside a camera is in use that checks a 20 cm × 20 cm area. In the background an AI based software is in use that evaluates rather there is a damage or not. It does it based on examples that it got taught before. Furthermore, with this it's possible to identify letters on the barrel that helps to identify the barrel number and type.

To hold these elements a mount for the robot arm was developed for 3D-printing (Figure 5 (A)). This makes it possible to keep both elements on the robot arm without a tool switcher by a small footprint a low usage of material. For the camera it's recommended to have concentrated and balanced lightning. Therefore, a second 3D-Printing piece was developed that fits onto the screw holes of the camera with the same curvature as the barrels (Figure 5 (B)). The complete setup can be seen in Figure 5 (C).

3.2 Thermography

For an initial proof-of-concept we investigated two curved cuts from standard 200 L steel drums commonly used for low- and intermediate-level radioactive waste storage. They preserved the original circumferential curvature of the drum; overall

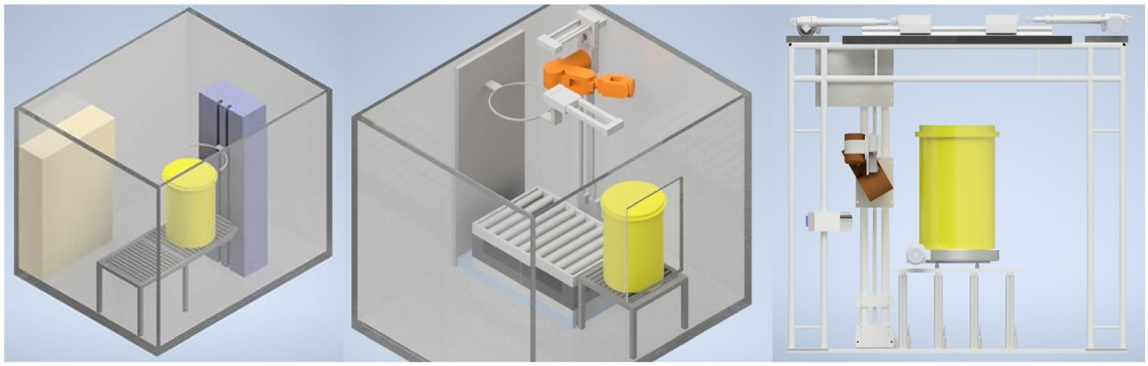

Figure 4: Design variants for an improved EMOS design. (A) Variant with lift, (B) Variant with lifting table, (C) Current planning status.

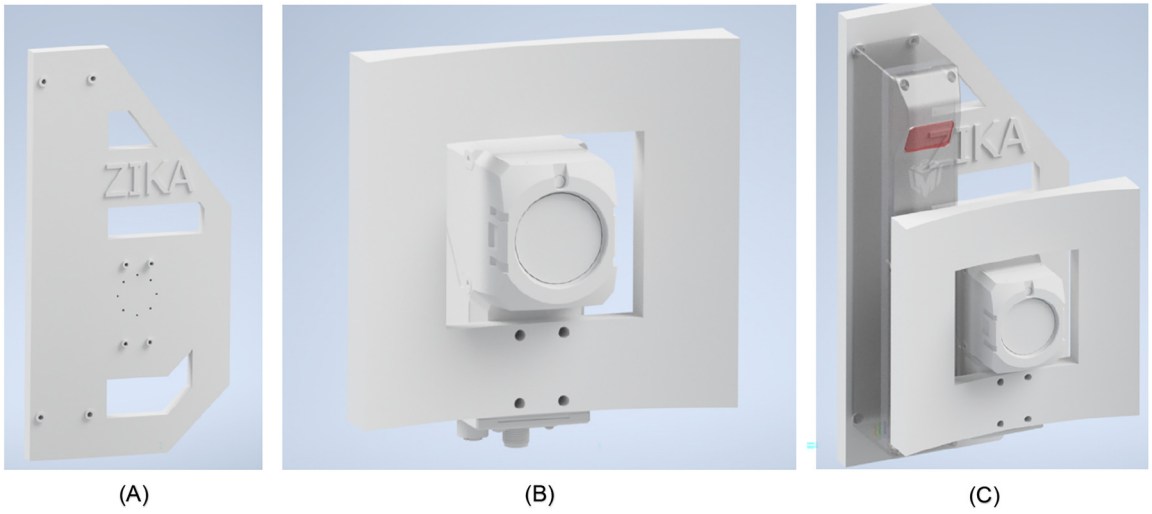

Figure 5: Improved optical inspection attachment. (A) Mount for robot, (B) Camera with light piece, (C) Complete setup.

planform dimensions were approximately 300 × 165 mm with a nominal wall thickness of 2.0 mm (ferritic/carbon steel, exact composition unknown) and an exterior paint coating of unknown formulation and thickness. The painted surface exhibited realistic field artefact – scratches, local paint inhomogeneity, slight geometric waviness, dirt, and weld-related irregularities – intentionally retained to reflect practical inspection conditions and to stress-test processing and automation.

Artificial subsurface defects were introduced as flat-bottom holes (FBHs) machined from the inner (concave) side to emulate internal corrosion pits. Each FBH was a cavity with depth of approximately 1.0 mm (i.e., ≈ half the 2 mm wall thickness).

Two specimens were prepared:

– Four-FBH cut: FBH diameters of 2, 4, 6, and 9 mm (depth ≈ 1.0 mm). This specimen served to benchmark detectability of lateral sizes at fixed depth (Figure 6 (A)).
– Fifteen-FBH cut: 15 defects with diameters 4, 6, and 9 mm (multiple repeats per size) at the same nominal depth. This specimen was used to assess repeatability, robustness to surface variability, and to develop/validate machine-learning classifiers (Figure 6 (B)).

3.2.1 Setup description

In our setup shown in Figure 8 (A), we employed a high-power diode laser source centered at =940 ± 5 nm with electronically controlled output up to 500 W and a specified 10–90 % modulation rise time below 100 µs. A refractive beam-shaping optic produced a quasi-top-hat square spot of 68 × 68 mm^2 at a 300 mm working distance. The beam was directed normal to the painted exterior surface via a mirror/beam splitter arrangement; a fast photodiode monitored the optical output for timing and phase reference. Thermal responses were recorded by an MWIR camera (InfraTec

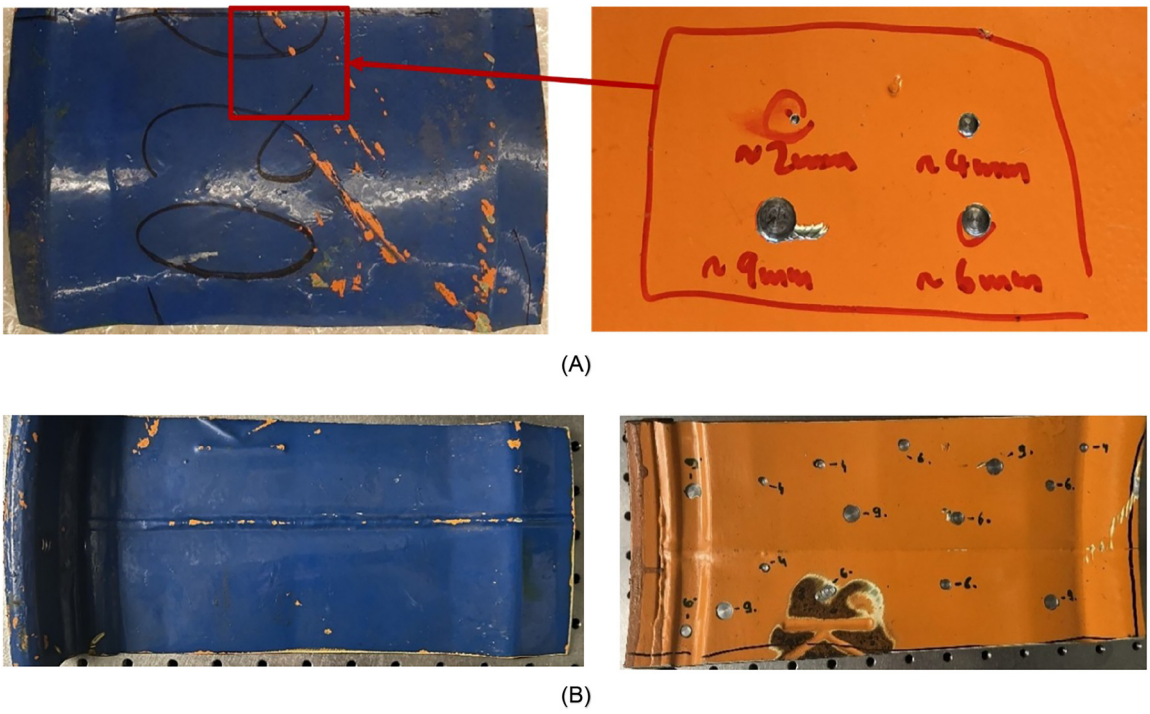

Figure 6: Different barrel cutouts used as test specimens. (A) Barrel cutouts containing four FBHs, (B) Second cutout containing 15 FBHs. Reproduced from (Averin et al. 2025).

ImageIR 9300, 1,280 × 1,024 px, effective spatial resolution of 70 µm/pixel) at up to 100 Hz in full frame. Normal positioning of the barrel cuts relative to the laser beam was achieved using the robotic arm illustrated in Figure 4 (A). Initially, the barrel cuts were scanned with a laser scanner. For each measurement region, the local surface orientation was determined by calculating a principal normal, defined as the eigenvector corresponding to the smallest eigenvalue obtained from a principal component analysis (PCA) of all surface normals within the region. An example of the resulting principal normal map for the fifteen-FBH cut is presented in Figure 8 (A). The robotic arm then aligned each region such that the surface was oriented normal to both the camera and the laser beam, based on the calculated principal normal.

3.2.2 Experiment with laser thermography

We first evaluated pulsed excitation at 500 W with pulse durations of 200ms and 500 ms (100 Hz sampling). For a 68 mm × 68 mm spot, these settings correspond to nominal energy densities of approximately 2.2 J cm^{-2} (200 ms) and 5.4 J cm^{-2} (500 ms), respectively. Each sequence included at least 100 pre-pulse frames to estimate and subtract a pixel wise baseline (temporal mean), followed by post-pulse acquisition spanning several seconds. Figure 7 (A) illustrates the resulting apparent temperature change curves (emissivity was taken to be 1 because in this study we focused on comparative analysis). After subtracting the background (calculated as the pixel-wise mean of 100 frames immediately before the heating event), the sequences were processed.

Processing comprised:

- Thermal Signal Reconstruction (sixth-order polynomial fit in log-log domain) with derivative products,
- Pulse Phase Thermography (FFT-based amplitude and phase),
- Principal Component Thermography (rank-5 reconstruction from SVD).

Defect contrast was enhanced by adjusting global intensity thresholds. Results presented in Figure 9 (A) clearly indicate defect visibility: FBHs of 4 mm to 9 mm diameter were consistently apparent in TSR, PPT phase, and the leading PCT components; the 2 mm FBH was not detected in any of the postprocessed images. Nonetheless, several non-defect features (scratches, paint inhomogeneity, slight geometric waviness) made defect localization ambiguous, prompting further investigation using LIT.

Lock-in thermography experiments were performed utilizing the same laser source. For the analysis, the sample was assumed to be ferritic steel (grade 1.4016). The phase function was plotted for a 5 mm depth range to show function saturations for different frequencies. The plot indicated

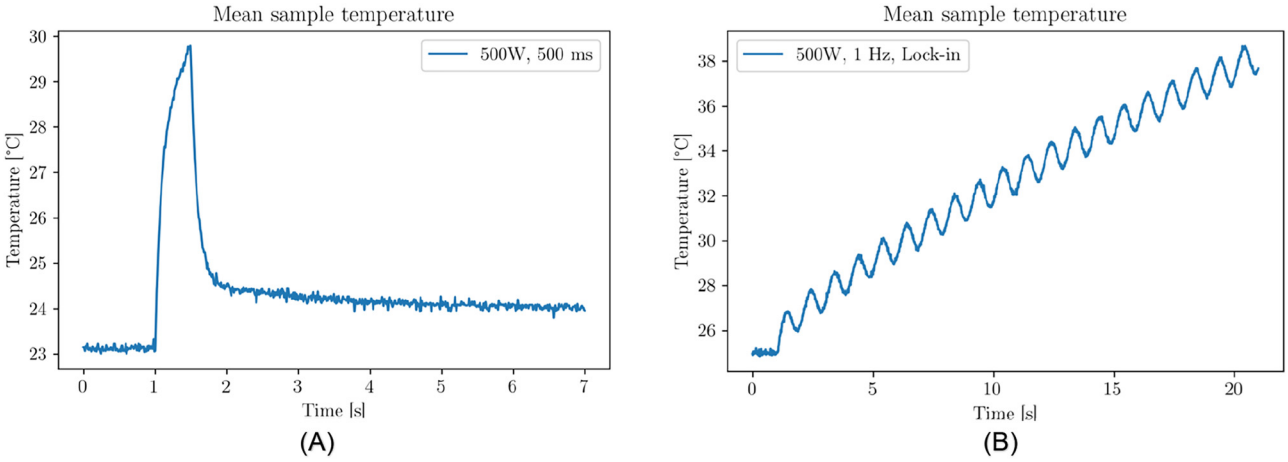

Figure 7: Sample surface temperature evolutions for different excitation strategies. (A) Pulsed excitation, (B) Sinusoidal excitation. Reproduced from (Averin et al. 2025).

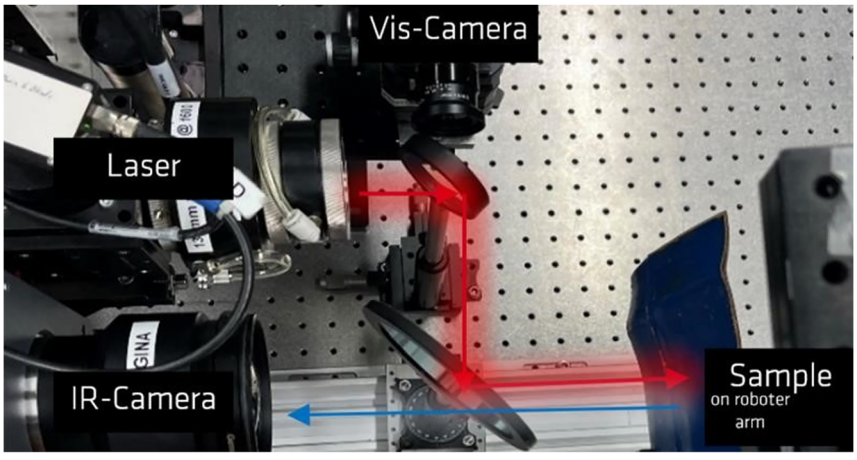

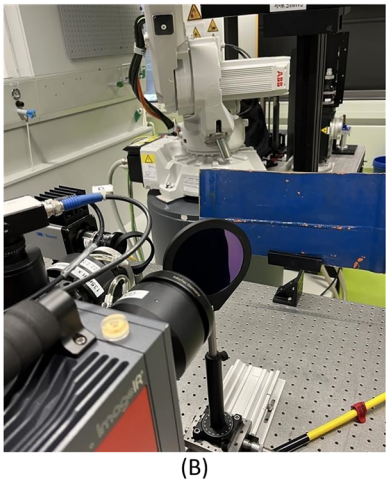

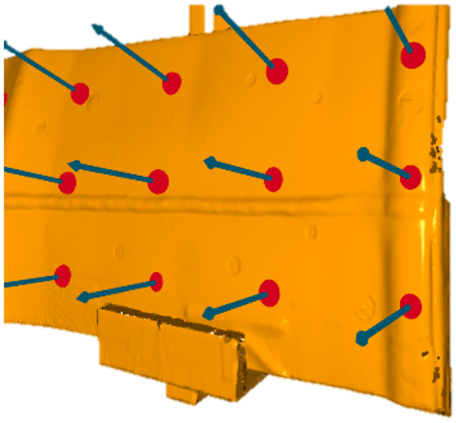

Figure 8: Experimental setup for examining the feasibility of thermographic testing. (A) BAM setup for laser thermography, (B) Robotic arm holding the sample, (C) Laser scanning result of a barrel cutout with principal normal vectors for all measurement regions. Reproduced from (Averin et al. 2025).

that a 1 Hz excitation frequency was optimal, saturating at a depth of 2 mm. At 1 Hz, the phase difference between a 2 mm (barrel wall) and a 1 mm (FBH) defect was approximately 0.43 rad (Figure 10).

Lock-in experiments were conducted using a 350 W laser operated in a sinusoidal heating mode at modulation frequencies of 0.3 Hz, 1.0 Hz and 1.5 Hz, with a heating duration of 20 s.

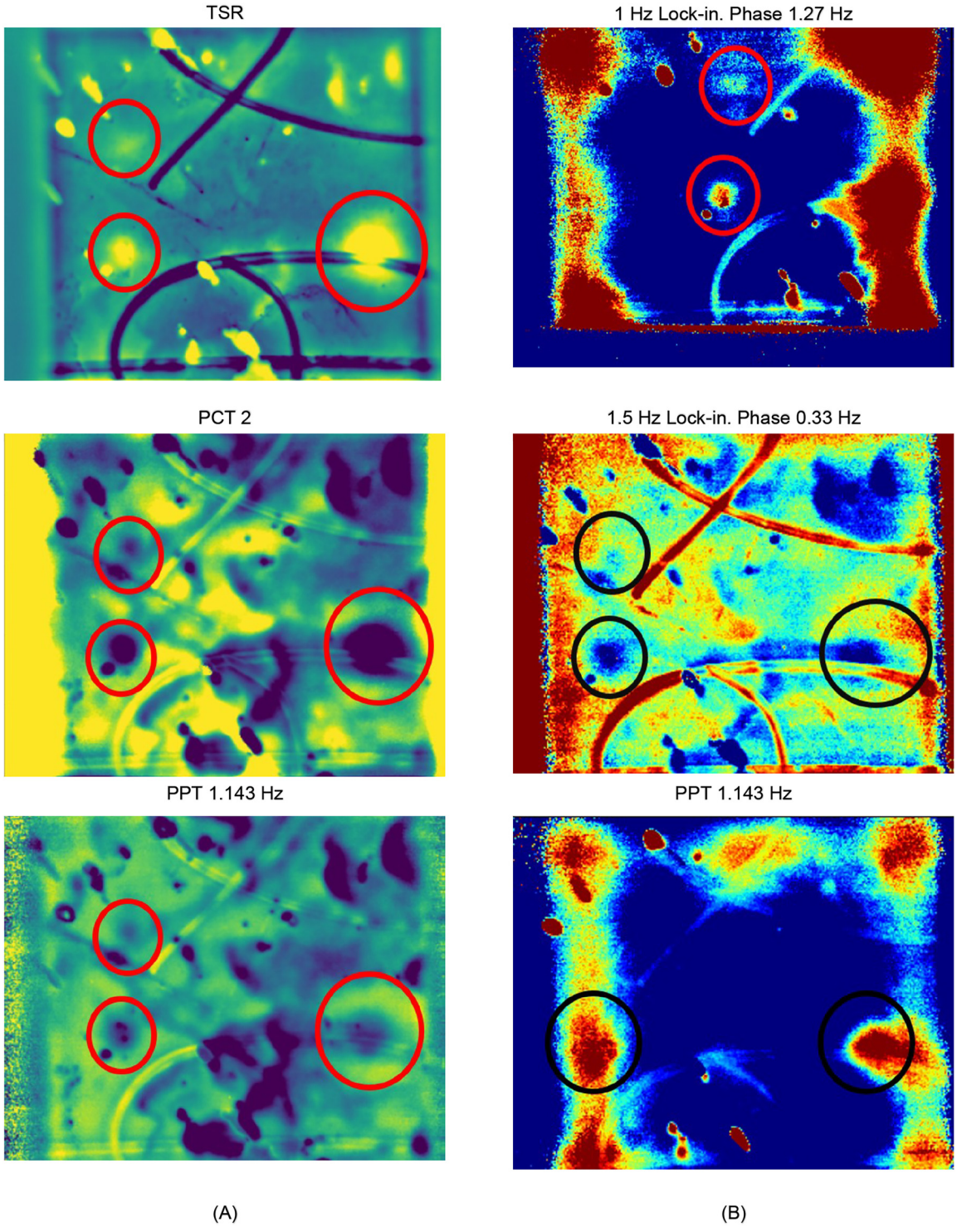

Figure 9: Best post-processed images for various laser thermography methods. Defects are circled. (A) Pulsed excitation, (B) Sinusoidal excitation. Reproduced from (Averin et al. 2025).

After DC component removal, phase data were extracted via fast Fourier transform (DFT) and analyzed; representative results are shown in Figure 9 (B). The analysis indicated that the overall quality of lock-in thermography was comparable to that of pulse thermography (PT) for the 1.27 Hz phase image at 1 Hz excitation. Additional frequency ranges were identified that could resolve certain defects; however, these were found to be highly susceptible to edge effects, with lateral heat diffusion leading to inconsistencies and some defects remaining undetectable. Due to the

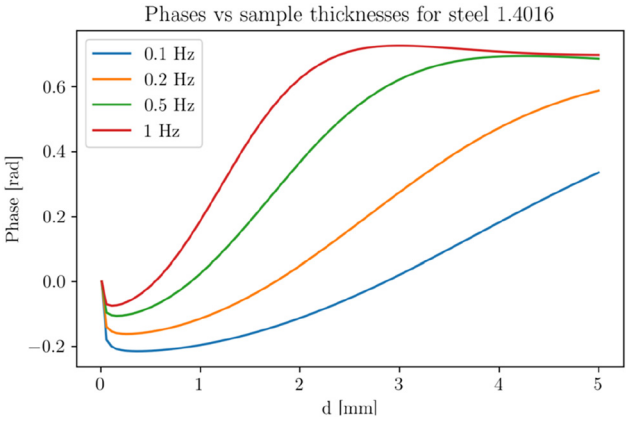

Figure 10: Evaluation of optimal frequencies for lock-in thermography reproduced from (Averin et al. 2025).

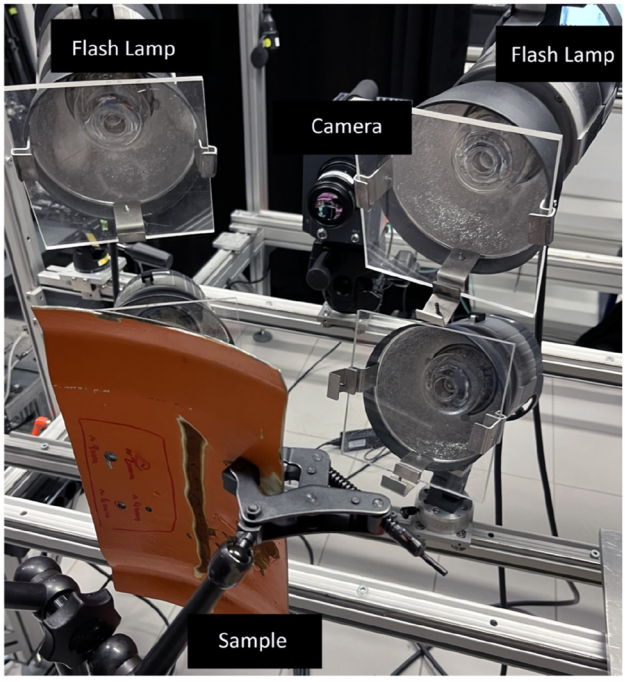

Figure 11: BAM setup for flash thermography reproduced from (Averin et al. 2025).

instability and frequency sensitivity of the lock-in approach, pulse thermography was determined to be the more robust and efficient method for laser thermography — providing reliable defect detection without additional computational processing and with shorter measurement times, a critical factor for large-scale inspection of thousands of barrels.

3.2.3 Experiments with flash thermography

The motivation for exploring flash thermography was twofold: to reduce the cost of the final test setup and to investigate the sample response using an alternative heat source. The same IR camera and acquisition parameters were employed; however, the heat source was replaced with four flash lamps, each providing a power density of 0.3 W cm^{-2}. This power density corresponds to a distance of 300 mm from the sample, where the lamps were positioned. Each lamp was equipped with an acrylic glass sheet serving as a short-pass filter, ensuring that the majority of the emitted energy remained within the visible and short-wave infrared spectrum (up to 1.5 µm). The lamps have a fullwidth at half-maximum (FWHM) pulse duration of approximately 2.6 ms and were focused directly on the defect area. The experimental setup is illustrated in Figure 11.

In these experiments, the average sample surface "apparent temperature" rose to approximately 69.8 °C at the maximum frame. The pulsed thermal image sequence was subsequently processed using PCT, TSR, and PPT, with the most informative results presented in Figure 12.

Under the tested conditions, flash thermography underperformed relative to laser-pulse excitation. After contrast enhancement, a maximum two FBH was reliably discernible in the processed images. The likely causes are practical rather than fundamental:

– Temporal undersampling: The 2.6 ms flash is much shorter than the 10 ms camera sampling interval (100 Hz). Early – time transients-most informative for

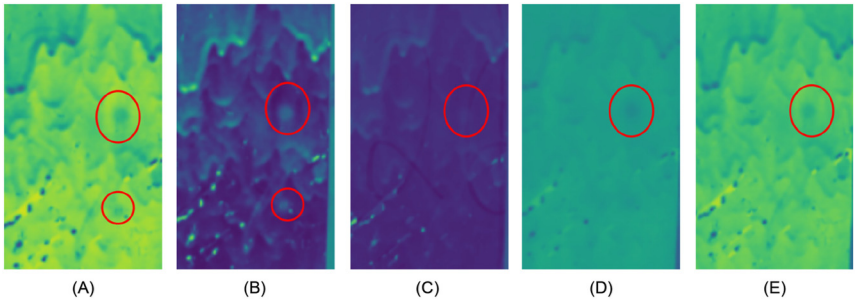

Figure 12: Postprocessed ash thermography images reproduced from (Averin et al. 2025).

shallow defects – were not adequately captured, reducing the effectiveness of TSR and PPT.
- Spatial non-uniformity: Multi-lamp illumination on a curved, painted surface produced gradients, hot spots, and shadows that were only partially mitigated by phase/PCT processing.
- Spectral coupling: Broadband visible light couples variably through paint pigmentation and gloss, increasing spatial variability compared with the narrow band near-IR laser spot.

Given these limitations and the superior robustness and cycle time obtained with the shaped 940 nm laser pulses, we prioritized laser thermography for the remainder of the study. Flash thermography remains attractive from a cost and maintenance perspective and may be revisited after targeted optimizations. Overall, the flash thermography setup lags behind the laser-based approach in result quality. With enhanced contrast, only one defect is visible in post-processed data. Consequently, further research focused exclusively on laser thermography, with flash thermography reserved for subsequent comparative analyses after successful optimization of the laser method.

3.3 Process in ZIKA

A forklift truck places the barrel to be tested on the lifting columns with a platform and a driven turntable through a roller door. In the next step, the barrel is raised with the lifting columns so that the barrel lid is at gripper height, which is brought together in parallel by linear units. This centers the barrel through the lower shells, and when the lifting columns are lowered, it is held in place by the upper shell. A robot, which is also connected to a linear unit, then moves under the barrel bottom and grips it using the same system as in EMOS (Figure 13 (A)). In the next step, the lifting columns move up again and the grippers move apart again, allowing the barrel to be picked up again and the lifting columns to move down far enough for the thermography system, in combination with the rotating plate, to examine the lower part of the barrel for internal corrosion (Figure 13 (B)). Thermography was selected as a non-destructive testing method as a result of the BAM tests. The system had proven to be the most reliable and reproducible in the tests.

After measuring the lower area, the lifting columns move to the lowest level to measure the upper area of the shell (Figure 13 (C)). Once this measurement is complete, the robot moves into position to capture the shell and then into position to capture the lid. In the final step, the roller door opens again and the forklift can pick up the barrel again.

3.4 Results

So far, only the BAM experiments with thermography have produced demonstrable results, as the prototype is still under construction.

For automated defect classification, combined thermographic evaluation methods were initially used, which enabled initial artifact suppression through optimized image fusion. Building on this, decision tree ensembles, in particular random forests, achieved the highest detection rate of all methods tested and identified all defects with

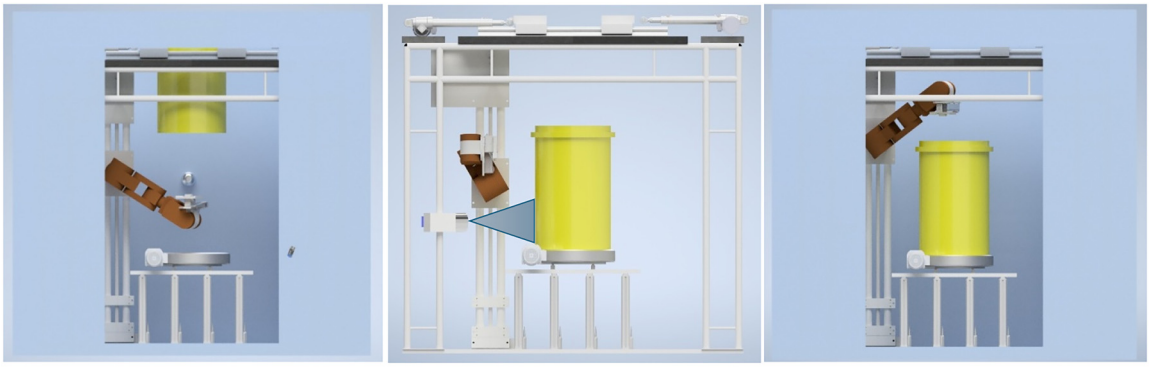

Figure 13: Visualization of the inspection process. (A) Checking the bottom, (B) Additional thermographic measurement step, (C) Checking the lid. (Averin et al. 2025).

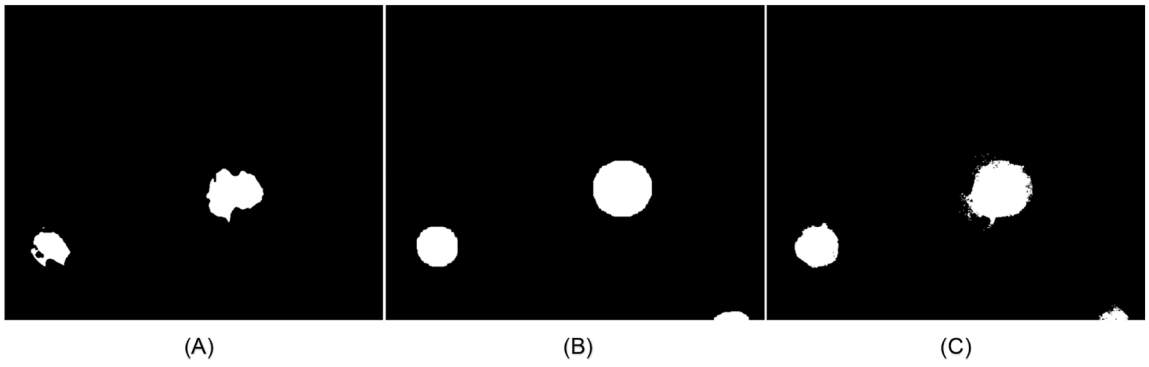

Figure 14: ML-based post-processing results of the thermographic data. (A) Decision tree result, (B) Ground truth data, (C) CNN result. Partly reproduced from (Averin et al. 2025).

minimal false alarms. In addition, trained convolutional neural networks also delivered robust results, but lagged slightly behind the random forest models. Both ML approaches consistently confirmed the relevance of specific PPT low frequencies and PCT components as the most important feature sources. Overall, the results show that ML-based fusion of thermographic feature spaces contributes significantly to the reliable differentiation of defects and surface-related artifacts (Figure 14).

4 Discussion

Even though laser thermography showed to be the preferred option in terms of reliability and resistance against reflection, flash thermography was chosen for this specific project they do not impose any additional requirements on potential users compared to the use of a laser thermography which would limit the use of this system.

For the camera and laser setup the change from EMOS to the smart camera improves the quality of the results as it's possible to clearly identify each single damage per barrel. For the lasers no changes were necessary as it already showed reliable results in EMOS.

5 Conclusion and outlook

During the course of the research project ZIKA, it has been shown that its possible to perform the barrel inspection in smaller footprint than in EMOS with more information about each barrel. This means a reduction from 20" High Cube Container to a 10" High Cube Container and knowledge about the specific damages and especially about potential internal corrosion instead of only knowledge about damages on the outside of a barrel. Furthermore, it could be confirmed that thermography is a reliable approach for detecting inner corrosion. By the beginning of 2026 the prototype is supposed to be ready for demonstration and use. From then the optimization process begins with the goal to evaluate the most efficient way for processing the data.

Research ethics: Not applicable.
Informed consent: Not applicable.
Author contributions: All authors have accepted responsibility for the entire content of this manuscript and approved its submission. N.H.: Conceptualization, Methodology, Investigation, Data curation, Formal analysis, Visualization, Writing – original draft, Writing – review & editing; A.A.: Investigation (thermography), Writing – review & editing, Proofreading; J.L.: Supervision, Investigation (thermography), Writing – review & editing, Proofreading.
Use of Large Language Models, AI and Machine Learning Tools: DeepL (improvement of language).
Conflict of interest: None declared.
Research funding: The research project Automated non-destructive internal corrosion detection on radioactive drums (ZIKA) is funded by the German Federal Ministry of Research, Technology and Space (BMFTR) and supported by the Society for Plant and Reactor Safety (GRS) GmbH. It is part of the sponsoring programme FORKA – Research for the dismantling of nuclear facilities and is listed under the funding code FKZ: 15S9446A.
Data availability: The data that support the findings of this study are available fromthe corresponding author, N.H., upon reasonable request.

References

Altenburg, S.J., Weber, H., and Krankenhagen, R. (2018). Thickness determination of semitransparent solids using flash thermography and an analytical model. *Quant. Infrared Thermogr. J.* 15: 95–105, https://doi.org/10.1080/17686733.2017.1331655.

Antons (2019). Thermografische Schichtdickenbestimmung von Oberflächenschutzsystemen. *Erhaltung von Bauwerken*.

Averin, A., Hirsch, P.D., and Lecompagnon, J. (2025). Automated thermographic inspection of radioactive waste drums. *Proc. SPIE, Thermosense: Thermal Infrared Applications XLVII* 13470: 134700Y, https://doi.org/10.1117/12.3052732.

BASE. (2024). Abfallarten. https://www.base.bund.de/de/zwischenlager/atommuell/abfallarten/abfallarten-atommuell.html#:~:text=Radioaktive%20Abfälle%20lassen%20sich%20unterscheiden%20in%20schwachradioaktive%20Abfälle%20(%20LAW%20)%2C,und%20hochradioaktive%20Abfälle%20(%20HAW%20).

Bernegger, R., Altenburg, S.J., and Maierhofer, C. (2020). Quantfication of delaminations in semitransparent solids using pulsed thermography and mathematical 1D models. *Int. J. Thermophys.* 41: 67, https://doi.org/10.1007/s10765-020-02642-7.

Bundesgesellschaft für Endlagerung (2019). *Radioaktive Abfälle*, https://www.bge.de/fileadmin/user_upload/Standortsuche/Wesentliche_Unterlagen/Poster/20191209_Radioaktive_Abfaelle.pdf.

Bundesgesellschaft für Endlagerung. (2023). *Aktueller Bestand*. https://www.bge.de/de/abfaelle/aktueller-bestand/.

Jonietz, F., Myrach, P., Suwala, H., and Ziegler, M. (2015). Examination of spot welded joints with active thermography. *J. Nondestr. Eval.* 35: 1, https://doi.org/10.1007/s10921-015-0318-4.

Matthies, Klaus. (1998). *Dickenmessung mit Ultraschall Klaus Matthies… [et al.] ; [DGZfP, Deutsche Gesellschaft für Zerstörungsfreie Prüfung, Hrsg.]*. DVS Verlag.

Schlichting, J., Brauser, S., Pepke, L.-A., Maierhofer, C., Rethmeier, M., and Kreutzbruck, M. (2012). Thermographic testing of spot welds. *NDT&E Int.* 48: 23–29, https://doi.org/10.1016/j.ndteint.2012.02.003.